PFOS-induced excitotoxicity is dependent on Ca^{2+} influx via NMDA receptors in rat cerebellar granule neurons

Hanne Friis Berntsen[a,b,*], Cesilie Granum Bjørklund[a], Rønnaug Strandabø[c], Trude Marie Haug[d], Angel Moldes-Anaya[e,f], Judit Fuentes-Lazaro[g], Steven Verhaegen[a], Ragnhild Elisabeth Paulsen[g], R. Andrew Tasker[h], Erik Ropstad[a]

[a] Department of Production Animal Clinical Sciences, NMBU-School of Veterinary Science, P.O. Box 8146 Dep, N-0033 Oslo, Norway
[b] Department of Administration, Lab Animal Unit, National Institute of Occupational Health, P.O. Box 8149 Dep, N-0033 Oslo, Norway
[c] Department of Biosciences, University of Oslo, Oslo, Norway
[d] Department of Oral Biology, University of Oslo, Oslo, Norway
[e] R&D section, PET-center, University Hospital of North Norway (UNN), Tromsø, Norway
[f] Neurobiology Research Group, Department of Clinical Medicine, UiT The Arctic University of Norway, Tromsø, Norway
[g] Department of Pharmaceutical Biosciences, University of Oslo, Oslo, Norway
[h] Department of Biomedical Sciences, University of Prince Edward Island, 550 University Avenue, Charlottetown PEI, C1A4P3, Canada

ARTICLE INFO

ABSTRACT

Perfluoroalkyl acids (PFAAs) are persistent compounds used in many industrial as well as consumer products. Despite restrictions, these compounds are found at measurable concentrations in samples of human and animal origin. In the present study we examined whether the effects on cell viability of two sulfonated and four carboxylated PFAAs in cultures of cerebellar granule neurons (CGNs), could be associated with deleterious activation of the *N*-methyl-ᴅ-aspartate receptor (NMDA-R).

PFAA-induced effects on viability in rat CGNs and unstimulated PC12 cells were examined using the MTT assay. Cells from the PC12 rat pheochromocytoma cell line lack the expression of functional NMDA-Rs and were used to verify lower toxicity of perfluorooctanesulfonic acid (PFOS) in cells not expressing NMDA-Rs. Protective effects of NMDA-R antagonists, and extracellular as well as intracellular Ca^{2+} chelators were investigated. Cytosolic Ca^{2+} ($[Ca^{2+}]_i$) was measured using Fura-2.

In rat CGNs the effects of the NMDA-R antagonists MK-801, memantine and CPP indicated involvement of the NMDA-R in the decreased viability induced by PFOS and perfluorohexanesulfonic acid (PFHxS). No effects were associated with the four carboxylated PFAAs studied. Further, EGTA and CPP protected against PFOS-induced decreases in cell viability, whereas no protection was afforded by BAPTA-AM. $[Ca^{2+}]_i$ significantly increased after exposure to PFOS, and this increase was completely blocked by MK-801. In PC12 cells a higher concentration of PFOS was required to induce equivalent levels of toxicity as compared to in rat CGNs. PFOS-induced toxicity in PC12 cells was not affected by CPP.

In conclusion, PFOS at the tested concentrations induces excitotoxicity in rat CGNs, which likely involves influx of extracellular Ca^{2+} via the NMDA-R. This effect can be blocked by specific NMDA-R antagonists.

1. Introduction

Perfluoroalkyl acids (PFAAs) including perfluoroalkyl sulfonated (PFSA) and carboxylated (PFCA) acids are found in measurable concentrations in samples from humans and wildlife, due to widespread use in industrial as well as consumer products since the 1950's (Buck et al., 2011). In the industry they are used amongst others as surfactants, antireflective coatings for photolithography processes, etchants, lubricants and in ion-exchange processes (OECD, 2009), whereas in consumer products they may be found in paint and inks, in food contact papers, impregnation sprays, ski waxes and outdoor clothing (IVF Swerea, 2009; Kotthoff et al., 2015). They are slowly degradable (Haug et al., 2010; Holzer et al., 2009; Nilsson et al., 2010; Olsen et al., 2007), cross the blood brain barrier, and accumulate in the brain to a variable degree depending on their carbon chain length and functional group(s) (Ahrens et al., 2009; Eggers Pedersen et al., 2015; Greaves et al., 2013;

Maestri et al., 2006). Exposure to PFAAs has been associated with neurobehavioural effects in laboratory animals including mice, rats and zebrafish such as decreases in spontaneous motor ability, deranged spontaneous behavior such as rearing and locomotion, and lack of habituation, as well as increased swimming speed in fish (Chen et al., 2013; Johansson et al., 2008; Yang et al., 2009). In humans a recent study suggested that prenatal exposure to the PFAAs perfluorooctanesulfonic acid (PFOS) and perfluorooctanoic acid (PFOA) may be associated with a small to moderate effect on the neurobehavioural development of children and specifically an increase in hyperactivity (Hoyer et al., 2015), however more human studies are required due to large variability shown in published literature (Roth and Wilks, 2014).

Glutamate is considered the major excitatory neurotransmitter in the mammalian brain and spinal cord (Paoletti et al., 2013). Excitotoxicity refers to the process whereby neuronal death is induced by excessive rapid or prolonged activation of glutamate receptors (Fonnum and Lock, 2004), resulting in sustained elevation of free cytoplasmic Ca^{2+}, which in turn release more glutamate into the affected area. Excitotoxicity is assumed to be involved in several pathological conditions such as ischemic brain injury (after stroke or trauma) and neurodegenerative disorders (e.g. Alzheimer's disease and Huntington's disease) (Feng et al., 2004; Marini and Paul, 1992; Xia et al., 1995). In addition to the metabotropic glutamate receptors, there are three types of ionotropic glutamate receptors, the α-amino-3-hydroxy-5-methylisoxazole-4-propionic acid (AMPA), kainate and *N*-methyl-ᴅ-aspartate (NMDA) receptors (Fonnum and Lock, 2004; Li et al., 2004), which contain central ligand gated ion-channels (Fonnum and Lock, 2004), all three which have been implicated in glutamate neurotoxicity (Marini and Paul, 1992). Of these the NMDA receptor (NMDA-R) is assumed to play a major role in the mediation of neuronal death in primary cultures of nerve cells (Marini and Paul, 1992).

The NMDA-Rs consist of several subunits forming heterotetrameric complexes (Feng et al., 2004; Tarnok et al., 2008), and contain a channel largely permeable to Ca^{2+} (Paoletti et al., 2013). Functional NMDA-Rs are formed by the combination of GluN1 and at least one GluN2 subunit, or GluN1 in combination with GluN2 and GluN3 subunits (Iacobucci and Popescu, 2018; Kew and Kemp, 2005). Similar to the cerebellum *in vivo*, the expression of subunits in cultures of cerebellar granule neurons (CGNs) *in vitro* changes with time, and maturation of the neuronal cultures (Cebers et al., 2001; Vallano et al., 1996). Due to these by others well documented and previously reported time-dependent changes in NMDA-R subunit expression, experiments in the present study were conducted in CGNs at various time-points, and neuronal cells exposed at days *in vitro* (DIV) 14 were assumed to express more mature receptors than cells exposed at DIV 0 or 8. This was however not verified by gene or protein analysis.

Granule cells are the most abundant neuronal cell type in the cerebellum (Gallo et al., 1982), they are easy to isolate, and to use in *in vitro* studies. They have been in use for several decades, and have been applied in many studies examining mechanisms of excitotoxicity. CGNs may be cultured to a high purity, express excitatory glutamate receptors, and produce and release L-glutamate (Kramer and Minichiello, 2010) and thus make, in addition to hippocampal and cortical cultures, a good model for the study of glutamatergic functions. Whereas the cerebellum earlier was assumed to be involved mainly in the planning and execution of movements, studies have shown that it is largely associated with cerebral networks involved in cognition (Buckner, 2013). Studies of children with malformations of the cerebellum find associations with neurophsychological deficits affecting executive functions, visuospatial and linguistic abilities, as well as with affective and social disorders, and autistic syndromes (Volpe, 2009). Exposure to certain POPs have been associated with an increased risk of autism spectrum disorders (Schmidt et al., 2014). Changes in the expression of ionotropic glutamate receptors have been observed in autism, and an upregulation of NMDA-R GluN1 subunit protein levels has been

observed in post-mortem samples from the human cerebellum (Rojas, 2014). In animal models of autism overexpression of GluN2B has also been observed (Rojas, 2014). In the cerebellum the migration of granule cells from the external germinative layer to the internal granule cell layer is dependent on the NMDA-Rs, where the GluN2B subunits are especially important (Akazawa et al., 1994; Llansola et al., 2005; Tarnok et al., 2008; Watanabe et al., 1994).

Previous studies using inhibitors of the NMDA-R function have indicated an involvement of this receptor in death of cultured CGNs induced by halogenated hydrocarbons such as the polychlorinated biphenyls (PCBs) (Mariussen et al., 2002), as well as the brominated flame retardant, tetrabromobisphenol A (TBBPA) (Reistad et al., 2007). We have previously reported that viability in cultures of CGNs exposed to six different PFAAs (perfluorohexanesulfonic acid (PFHxS), PFOS, PFOA, perfluorononanoic acid (PFNA), perfluorodecanoic acid (PFDA) and perfluoroundecanoic acid (PFUnDA)) is affected by carbon chain length and the functional groups attached to the perfluorinated molecular backbone (Berntsen et al., 2017). In the present study the initial aim was to investigate the possible involvement of the AMPA/kainate- and NMDA-Rs in PFAA-induced reductions in viability of CGNs using the same six compounds.

After the initial studies conducted with the six different PFAAs we chose to focus our remaining studies on PFOS. For comparative purposes we also included PFOA in some, but not all of the experiments. PFOS and PFOA both have 8 carbon atoms in the molecular backbone structure, but have different functional groups attached. Whereas PFOS has a sulfonate group, PFOA contains a carboxyl group (Fig. 1).

We have previously reported that CGNs exposed at DIV 8 to concentrations of PFOS and PFOA inducing equipotent effects after 24 h exposure, show very different time-curves for cytotoxicity induction. Whereas PFOS induced most of its toxicity within 1 h of exposure, PFOA did not induce significant effects on viability until after 12 h exposure (Berntsen et al., 2017), which may indicate different mechanisms of action. For the second part of the experiments the aim was to investigate how PFOS and PFOA affected the viability of CGNs at different stages of maturation. Further, time-dependent effects of intracellular and extracellular calcium chelation on PFOS- and PFOA-induced effects on viability were investigated. Finally, the effects of PFOS and PFOA exposure on cytosolic calcium concentration were assessed. Cells from the PC12 rat pheochromocytoma cell line reportedly lack the expression of functional NMDA-Rs (Edwards et al., 2007) and were exposed to concentrations within the same range as used in the CGN experiments, to verify lower toxicity of PFOS in cells not expressing NMDA-Rs.

2. Materials and methods

2.1. Chemicals and reagents

1,2-bis(o-aminophenoxy)-ethane-N,N,N-N′-tetraacetic acid tetraacetoxymethyl ester (BAPTA-AM, ≥ 90%), was obtained from Calbiochem (San Diego, CA, USA). Basal medium Eagle (BME), Dulbecco's modified Eagle medium (DMEM), heat-inactivated foetal bovine serum (FBS), Glutamax-I supplement (200 mM), heat-inactivated horse serum and penicillin-streptomycin (100 IU/ml penicillin and 100 μg/ml streptomycin) came from GIBCO Life technologies (Paisley, UK). Perfluorohexanesulfonic acid potassium salt (PFHxS, > 98%) was purchased from Santa Cruz Biotechnology, Inc. (Santa Cruz, CA, USA). Albumin from bovine serum (BSA, ≥ 96%), cytosine β-D-arabinofuranoside (ARA-C, ≥ 90%), deoxyribonuclease I from bovine pancreas (DNAse), dimethyl sulfoxide (DMSO, ≥ 99.9%), ethylene glycol-bis(2-aminoethylether)-*N,N,N′*,N′-tetraacetic acid (EGTA, ≥ 97.0%), memantine hydrochloride (memantine, ≥ 98%), +/-MK-801 hydrogen maleate (MK-801), perfluorooctanesulfonic acid potassium salt (PFOS, ≥ 98%), perfluorooctanoic acid (PFOA, 96%), perfluorononanoic acid (PFNA, 97%), perfluorodecanoic acid (PFDA, 98%), perfluoroundecanoic acid (PFUnDA, 95%), poly-ʟ-lysine
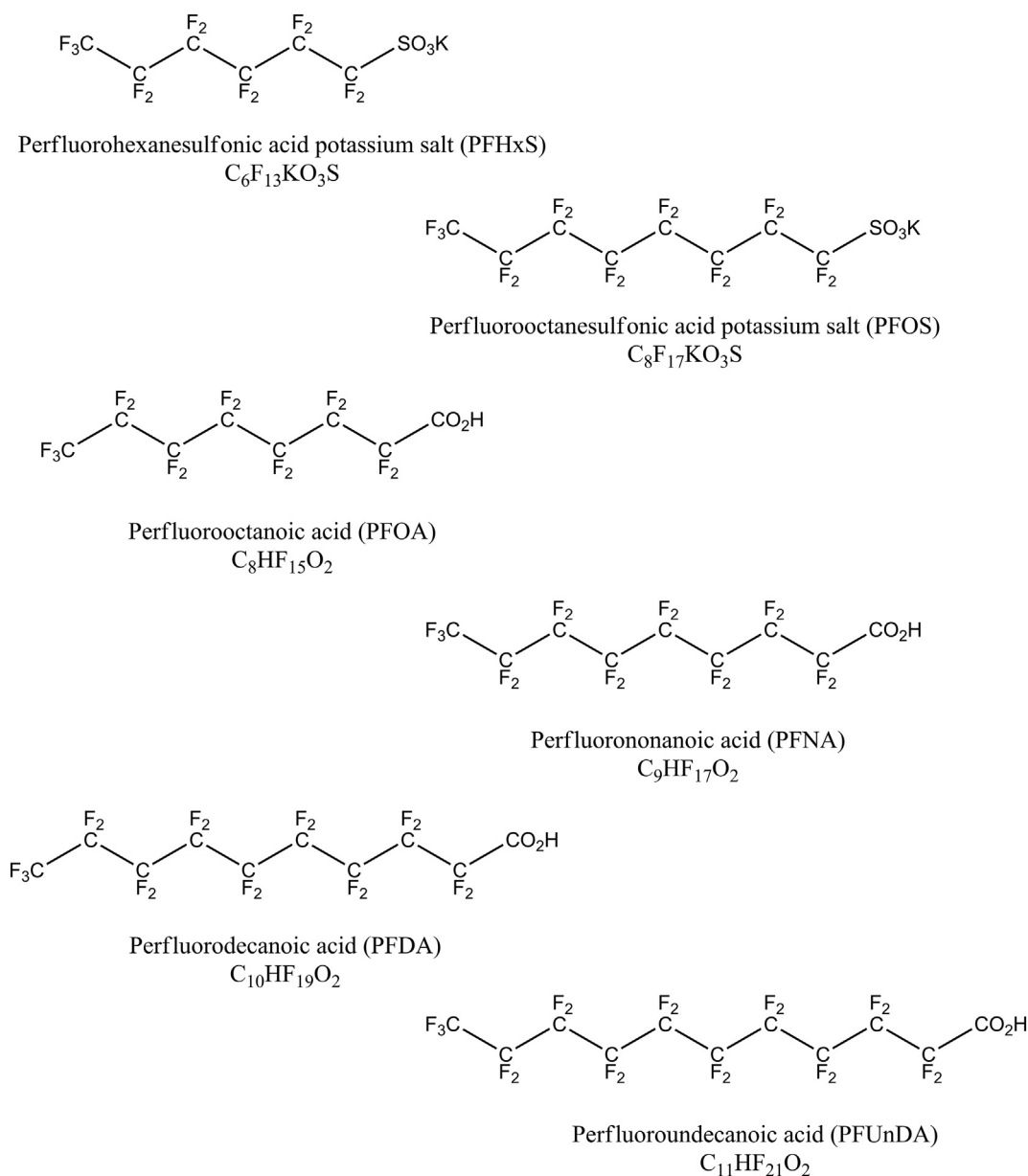
Fig. 1. The chemical structures of the six different PFAAs. Adapted from (Berntsen et al., 2017).

hydrobromide (M_w > 70,000), 3-(4,5-dimethylthiazol-2-yl)-2,5-diphenyl tetrazolium bromide (MTT, 98%), trypsin type I from bovine pancreas and trypsin inhibitor from *Glycine max* (soybean) type I−S were purchased from Sigma-Aldrich (St.Louis, MO, USA). 3-((R)-2-Carboxypiperazin-4-yl)-propyl-1-phosphonic acid (CPP, ≥ 98%), 2,3-dioxo-6-nitro-1,2,3,4-tetrahydrobenzo[*f*]quinoxaline-7-sulfonamide disodium salt (NBQX, ≥ 98%) was from Tocris Biosciences (Bristol, UK). All other chemicals and reagents used were obtained from standard chemical suppliers. Stock solutions of all relevant concentrations of PFAAs and BAPTA-AM were prepared by dissolution in DMSO, whereas CPP, MK-801 and memantine were dissolved in Milli-Q-water. The stocks were frozen, and thawed before each experiment so that the same stocks were used for all experiments. For EGTA a 0.5 M stock solution was made by dissolution of 1.9 g EGTA in 9 ml distilled water added 0.4 g NaOH to reach a pH of 7.5, followed by further addition of 1 ml distilled water. The stock solution was stored in the fridge and used for all the experiments involving EGTA.

2.2. Laboratory animals

For each isolation of cells, mixed-sex litters of 10 Wistar rat pups were obtained at 8 days of age from Taconic, Denmark. The pups were euthanised, without prior use of anaesthesia, by decapitation on the day of arrival, whereas the dam was euthanised with an intracardiac injection of pentobarbital under isoflurane anaesthesia, followed by opening of the thoracic cavity. All animal treatments were carried out in accordance with the Norwegian Animal Welfare Act and the Directive 2010/63/EU of the European Parliament and of the Council on the protection of animals used for scientific purposes. Efforts were made to minimise animal suffering and to reduce the number of animals used.

2.3. Isolation of rat cerebellar granule neurons

Primary cultures of post-mitotic cerebellar granule neurons were prepared as described in Berntsen et al. (2013) from rat pups at post-natal day (PND) 8. Cells from each isolation were diluted to an

approximate concentration of $1–1.2 \times 10^6$ cells/ml in BME, supplemented with 10% heat-inactivated FBS, 2.5 mM Glutamax, 100 IU/ml penicillin +100 μg/ml streptomycin, 25 mM KCl and 1% glucose (sBME), and transferred to 12 well poly-L-lysine treated (.01 mg/ml for 2 h, 1 ml per well) cell culture plates (Nunc, 1 ml cells per well) for the cytotoxicity experiments. For Ca^{2+} imaging cells were seeded in pre-coated poly-D-lysine 3.5 cm dishes with a central glass bottom of 1.4 cm in diameter (MatTek Corporation, 3 ml cells/dish). The cytostatic drug ARA-C was added to all plates after 24 h - at day 1 in vitro (DIV), giving a concentration of 10.3 μM in the cell medium, to prevent the replication of non-neuronal cells. Cells were then left undisturbed in a CO_2 incubator without medium change, at 36 °C and 5% CO_2 until DIV 8–9 or 14, when exposures were carried out. For CGN-cultures left until DIV 14 additional glucose (1 mg/ml) was also added to the medium as previously described by Schramm et al. (1990) for the maintenance of healthy cultures. In the present study, glucose was added approximately every third day as in de Luca et al. (1996) at DIV 7, 9 and 12. For all chemical exposures performed at DIV 8 or DIV 14 CGNs were exposed to toxicants in sBME, without FBS (sBME (− FBS)). For the exposure of cells at DIV 0, $2\times$ the normal concentration of cells ($2–2.4 \times 10^6$ cells/ml) in sBME were seeded in half the normal volume of medium (0.5 ml cells/well) followed by addition of $2\times$ the desired final concentration of toxicants/DMSO in additional medium (0.5 ml/well), giving a concentration of $1\times$ for the relevant toxicant in 1 ml medium/well. ARA-C was added at DIV 1 as usual. All exposures were performed in triplicate wells, and a mean value calculated for each concentration. Each experiment was repeated several times (depending on the experiment) in cell cultures isolated from cerebella at different days (cells from one isolation was counted as one independent replicate).

2.4. PC12 cells

Cells from the rat pheochromocytoma cell line PC12 were grown in DMEM supplemented with 10% FBS, 5% horse serum, sodium pyruvate (1 mM) and 100 IU/ml penicillin +100 μg/ml streptomycin, diluted to a concentration of 3.5×10^4 cells/ml and plated 100 μl/well in a 96-well, transparent, flat-bottom cell culture plate (Nunc). Cells were subsequently incubated for 24 h at 37 °C and 5% CO_2, followed by exposure to toxicants and inhibitors in supplemented DMEM for yet 24 h at 37 °C and 5% CO_2, before cell viability assessment with the MTT assay.

2.5. MTT cell-viability assay

The MTT assay was used for measurement of cell viability in the rat cerebellar neuronal experiments described in this paper. To verify the viability-results from the MTT assay, cells from all exposed wells in an experiment were also examined by phase contrast microscopy, prior to conducting the assay. The MTT assay was also used for cell viability assessment in PC12 cells. The MTT assay is based on the cleavage of the yellow tetrazolium salt MTT into the blue product formazan by the mitochondrial enzyme succinate dehydrogenase in living cells (Mosmann, 1983). In the assay, a reduction in the number of living cells results in a decrease in the amount of formazan produced as compared to the control, and indicate the degree of cytotoxicity induced. For the studies in rat cerebellar granule neurons, the assay was conducted as described in Berntsen et al. (2013), and dual wavelength absorbance measurements were performed at 570 and 690 nm in a VICTOR3 multilabel reader (Perkinelmer, Inc. Waltham, MA, USA). For the PC12 cells, after end of exposure, 10 μl of 5 mg/ml MTT solution in PBS was added to each well of the 96 well plate, with the exception of the wells left for background subtraction. The plate was subsequently incubated at 37 °C and 5% CO_2 for 3 h, before replacement of the MTT-solution with 100 μl DMSO/well for dissolution of the formazan salt. Absorbance was subsequently measured after 30 min at 570 nm in a CLARIOstar® microplate reader (BMG Labtech, Ortenberg, BW, Germany), and the average blank value from wells containing cells without MTT, was subtracted from the final optical density values obtained.

2.6. Mechanistic studies of the involvement of ionotropic glutamate receptors in PFAA-induced cytotoxicity

To examine the involvement of ionotropic glutamate receptors in PFAA-induced cytotoxicity, CGNs were exposed on DIV 8 to a single concentration of the PFSAs PFHxS (550 μM) and PFOS (60 μM) as well as the PFCAs PFOA (500 μM), PFNA (100 μM), PFDA (40 μM) and PFUnDA (30 μM) for 24 h, alone or in conjunction with the uncompetitive NMDA-R antagonist memantine (Volbracht et al., 2006), the high affinity uncompetitive NMDA-R antagonist MK-801 (Frankiewicz et al., 1996), or the competitive NMDA-R antagonist CPP (Fritz et al., 1996). Preliminary experiments with PFOS, and various concentrations of CPP were conducted to assess the effect of different concentrations of CPP. In addition, cells were co-incubated with the AMPA/kainate receptor antagonist NBQX (Mitsui et al., 2011). The concentrations of the PFAAs were based on concentration-response experiments described in a separate publication (Berntsen et al., 2017). Concentrations producing close to equipotent effects, i.e. some, but not full toxicity (60–80% reduction in cell viability), for all the PFAAs at 24 h, were selected. The concentrations of PFAAs used in the present study are higher than concentrations measured in the general population, and are more in the range of what may be found in occupationally high exposed workers. The concentrations of MK-801, memantine and NBQX were based on previous publications (Berntsen et al., 2013; Mariussen et al., 2002). The inhibitors were also tested alone to examine their effects on cell-viability in unexposed cells. To also assess involvement of mature NMDA-Rs in PFOS- and PFOA-induced cytotoxicity CGNs were exposed on DIV 14 to PFOS (60 μM) and PFOA (500 μM) for 24 h alone or together with memantine, MK-801, or CPP. The concentrations of the various inhibitors used as well as the number of independent experiments conducted are presented in Table 1.

2.7. PFOS and PFOA-induced cytotoxicity in CGNs at different stages of maturation

To assess potential differences in cytotoxicity of PFOS and PFOA in neuronal cultures at different stages of maturation, rat CGNs were exposed to increasing concentrations of PFOS and PFOA for 24 h at DIV 8 (10, 20, 40, 60, 80 and 100 μM PFOS, and 100, 200, 300, 400, 500 and 600 μM PFOA, $n = 5–7$) and DIV 14 ($n = 3$) before assessment of viability with the MTT assay. The concentration-response curves for PFOS and PFOA at DIV 8 have been published before (Berntsen et al., 2017), but are included in Fig. 4A and B for comparisons. To assess the effect of PFOS on immature NMDA-Rs, CGNs were also exposed to the same concentrations of PFOS in the presence of FBS, at cell isolation (DIV 0, $n = 3$) for 8 days until DIV 8, when viability was assessed.

Table 1
Concentrations and number of experiments conducted with each inhibitor alone or in combination with each PFAA in CGNs.

Exposure day in vitro (DIV)	Inhibitor	Concentration in μM	n
8	Memantine	3 and 6	5–7
8	MK-801	3	5–6
8	CPP	0.75 and 10	4–6
8	CPP + PFOS	0.75, 1.5, 3, 6 and 10	5
8	NBQX	10	5
8	All above inhibitors unexposed cells		5–6
14	Memantine	6	3
14	MK-801	3	3
14	CPP	10	3

n = number of independent experiments from separate cell isolates, each performed in triplicate

2.8. PFOS-induced toxicity in PC12 cells

To verify whether the PFOS-induced toxicity could be acting via the NMDA receptor, PC12 cells lacking the expression of functional NMDA-Rs (Edwards et al., 2007) were exposed to concentrations within the same range as used in the CGN experiments (12.5, 25, 50 and 100 μM). In addition, a higher concentration (200 μM) was used to ensure the likelihood of cytotoxicity induction ($n = 4$ for all). 200 μM PFOS was also tested in combination with CPP (0.75 and 10 μM, n = 3 for both).

2.9. Assessment of time-dependent effects of extracellular and intracellular Ca^{2+} chelation on cell viability after exposure to PFOS and PFOA

To assess effects of chelation of extracellular and intracellular Ca^{2+} CGNs were co-incubated for different time intervals with PFOS (60 μM) and PFOA (500 μM) alone, and in conjunction with the extracellular Ca^{2+} chelator EGTA (2 mM, 10, 30 and 60 min and 12 and 24 h, n = 4) and the intracellular Ca^{2+} chelator BAPTA-AM (10 μM, 10 and 60 min and 24 h, n = 4–6). Effects of EGTA and BAPTA-AM alone were also assessed (n = 4–6). At each time-point a DMSO control (0.1% for EGTA and 0.2% for BAPTA-AM) was included. The concentrations of EGTA and BAPTA-AM were based on previous experiments and publications (Berntsen et al., 2013; Reistad et al., 2007).

2.10. Effects of CPP on time-dependent changes in viability after PFOS and PFOA exposure

To assess acute effects of PFOS and PFOA exposure on CGN viability, and involvement of the NMDA-R in the induced toxicity, cells were incubated with PFOS (60 μM) or PFOA (500 μM) alone and in conjunction with CPP (10 μM) as well as CPP only (10 μM) and DMSO (0.1%) for 10 and 60 min (n = 4–5). Due to previous findings that this concentration of PFOA did not induce toxicity at these time-points (Berntsen et al., 2017), a higher concentration of PFOA (1000 μM) with and without CPP was also included (n = 3).

2.11. Measurements of cytosolic Ca^{2+} using Fura-2

Dishes containing CGNs were used at DIV 8–9 for Fura-2 measurements of cytosolic Ca^{2+} ($[Ca^{2+}]_i$) during 1 h exposure to toxicants and/or inhibitors. Cells were initially incubated with 5 μM of the fluorescent Ca^{2+} indicator Fura-2 AM in sBME ($-$ FBS) (1 ml/ dish), for 30 min at 37 °C and 5% CO_2. This was followed by washout of excess Fura-2 ester using sBME ($-$ FBS) (1 ml/dish), and further 30 min incubation in sBME ($-$ FBS) (1 ml/dish) at 37 °C and 5% CO_2. Subsequently for experiments another 1 ml of sBME ($-$ FBS) was added/dish. $[Ca^{2+}]_i$ imaging by dual excitation fluorometry was conducted as previously described in Strandabo et al. (2016) with modifications. In brief the dishes containing CGNs were mounted on an Olympus IX71 inverted microscope with objectives of high UV light transmittance (Olympus, Tokyo, Japan). Excitation light was provided by the use of a Lambda LS Xenon Arc lamp (Sutter, CA, USA). The wavelength of the light was altered between 340 and 380 nm with the aid of a Lambda 10–2 filter wheel, and the emission at 510 nm was recorded using a Hamamatsu ORCA ER camera (Hamamatsu Photonics, Hamamatsu, Japan). Ratio images were obtained at a frequency of 0.83 Hz. Exposure times varied according to the Fura-loading and were between 250 and 350 ms for 340 nm and between 50 and 150 ms for 380 nm excitation. The ratio between the emission at the two excitation wavelengths (F340/F380) reflects $[Ca^{2+}]_i$, and an increase in the ratio corresponds to an increase in $[Ca^{2+}]_i$. In the present study, exposures were performed by adding 1 ml of sBME ($-$ FBS) containing $3\times$ the desired final concentration of toxicants or sBME ($-$ FBS) only, to the dish already containing 2 ml of sBME ($-$ FBS). Measurements were taken before addition of toxicants (time point 0), followed by measurements at 30 and 60 min post treatment. For studies of cells co-treated with an inhibitor, this was

added 5 min prior to the addition of toxicants. Measurements of $[Ca^{2+}]_i$ were taken before addition of the inhibitor, after 5 min incubation with inhibitor alone (time-point 0), and 30 and 60 min after addition of toxicant. For each time-point, measurements of $[Ca^{2+}]_i$ were obtained from 5 cells in 4 random areas of each dish. For calculation of effects and statistical testing, an average value was calculated for the 20 observations obtained at each time-point. To correct for inter-experimental variability in baseline Ca^{2+} levels prior to treatment with toxicants, the average $[Ca^{2+}]_i$ value for the 20 cells obtained 30 and 60 min after treatment was expressed as % of the average $[Ca^{2+}]_i$ value obtained prior to treatment at time-point 0 (set to 1). In the case of the inhibitor studies the average values from 30 and 60 min were expressed as % of the average value obtained after 5 min incubation with the inhibitor. CGNs in the present study were treated with 60, 100 and 300 μM PFOS and PFOA for 60 min (n = 4–5). Due to the absence of an increase in $[Ca^{2+}]_i$ after PFOA treatment as compared to control cells, the effect of a higher concentration of PFOA and PFOS (1000 μM) was also examined (n = 4). To further examine whether the increase in $[Ca^{2+}]_i$ could be the result of influx via the NMDA-R, CGNs were preincubated with the NMDA-R channel blocker MK-801 (3 μM), before addition of PFOS or PFOA (300 μM of both) in conjunction with MK-801 (3 μM) or sBME ($-$ FBS) only ($n = 6$–8).

2.12. Statistical analysis

Statistical analyses and calculations were carried out using GraphPad Prism 7. For the assessment of significant alterations in viability in rat CGNs treated with the different PFAAs and MK-801, or NBQX, as compared to the PFAA alone, a two-tailed paired *t*-test was used, due to the comparison of two groups. For treatment with memantine or CPP, as well as treatment with inhibitors in rat CGNs at DIV 14, a repeated measure one-way ANOVA with a Dunnett's post hoc test was used due to comparison of several groups. Effects on cell viability after treatment of rat CGNs at DIV 8 with inhibitors only, effects on viability after exposure of rat CGNs to PFOS or PFOA at DIV 0, 8 and 14, effects on viability in PC12 cells after treatment with PFOS as compared to treatment with 0.1% DMSO, in addition to comparison of effects of treatment of PC12 cells with PFOS alone or together with CPP were assessed with one-way ANOVAs and Dunnett's post hoc tests. In all the studies where effects of exposure were examined at various time-points, significant differences were tested using a two-way ANOVA, with a Tukey-Kramer post hoc test. In all the experiments conducted, a *p*-value of < .05 was regarded as statistically significant. Best fit concentration-response curves for cell-viability were obtained by non-linear regression in PRISM 7. Concentrations were log transformed prior to analysis. A 4-parameter variable slope model was used with the bottom value constrained to 0 to improve fit.

3. Results

3.1. Mechanistic studies on the involvement of ionotropic glutamate receptors in PFAA-induced cytotoxicity

Three inhibitors were used for screening of the involvement of NMDA-Rs in PFAA-induced effects on viability in CGNs. The results are summarised in Fig. 2. MK-801 significantly improved viability after co-exposure with PFHxS and PFOS by 15 and 40 percentage points ($p < .05$ and .01, respectively), whereas in conjunction with PFOA and PFNA, viability was significantly reduced by 25 and 14 percentage points ($p < .05$) (Fig. 2A). No effects were observed for the PFDA- and PFUnDA-induced cytotoxicity. After co-incubation with 3 and 6 μM memantine, significant alterations in viability were detected as compared to PFAA exposure only (Fig. 2B). For PFHxS (ANOVA ($F_{2,5} = 12.7$, $p < .01$)) viability increased by 14 and 20 percentage points ($p < .05$ and .01, respectively), for PFOS (ANOVA ($F_{2,5} = 33.2$, $p < .01$)) by 22 percentage points for both concentrations ($p < .001$)
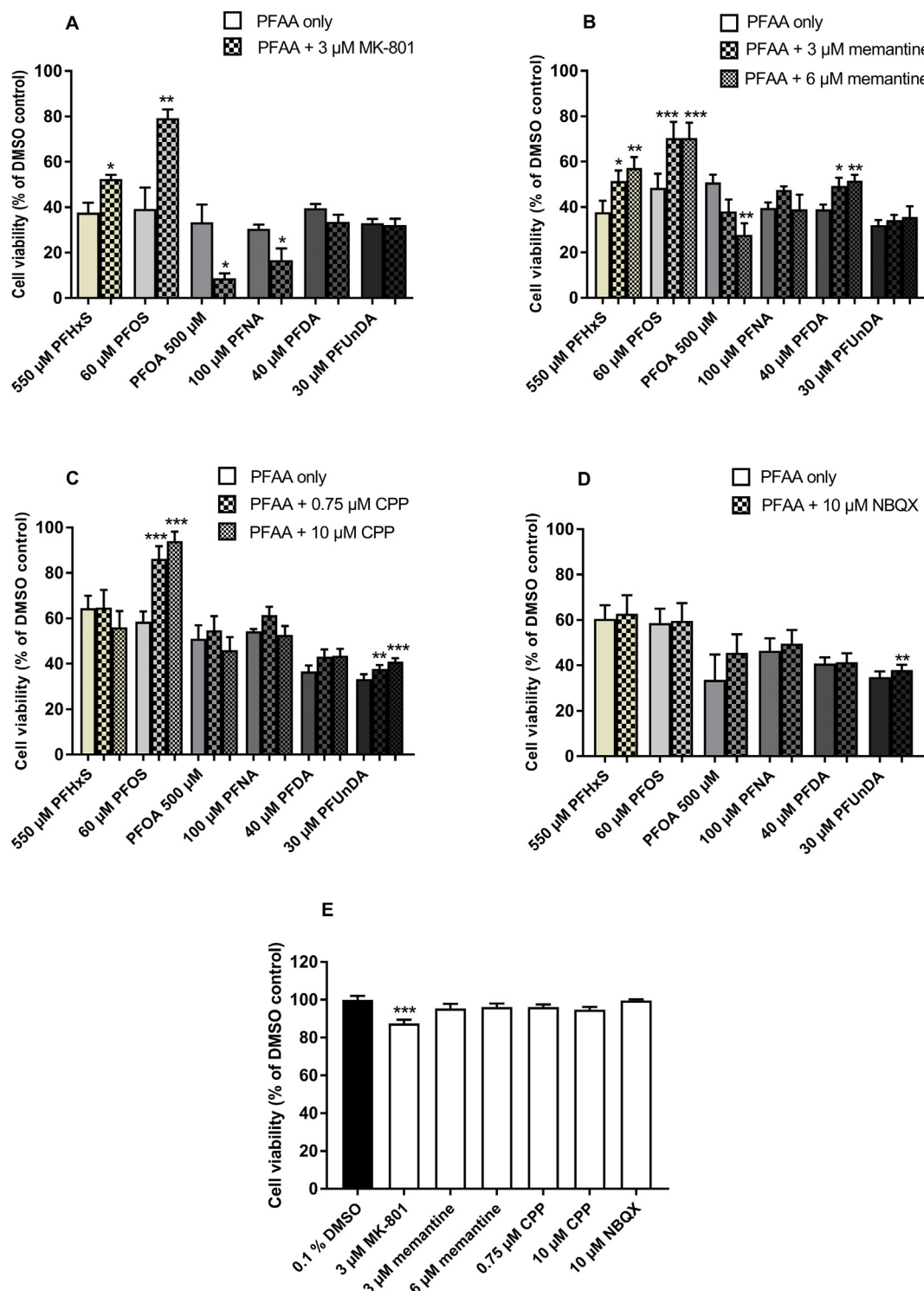
Fig. 2. Neuroprotective effects of ionotropic glutamate receptor antagonists on PFAA-induced cytotoxicity at day 8 *in vitro*. Viability was assessed with the MTT assay after 24 h exposure of rat CGNs at day 8 *in vitro* to the six PFAAs alone and in conjunction with A) MK-801 (n = 5–6 experiments from separate cell isolates), B) memantine (n = 5–7 experiments from separate cell isolates), C) CPP (n = 4–6 experiments from separate cell isolates) and D) NBQX (n = 5 experiments from separate cell isolates). E) The effects of inhibitors only on cell viability was also assessed (n = 5–6 experiments from separate cell isolates). All values are relative to the 0.1% DMSO control in each experiment (defined as 100%). *,** and *** indicate statistically significant differences of $p < .05$, $p < .01$ and $p < .001$, respectively between CGNs treated with the PFAAs alone and together with the various inhibitors, or between cells treated with 0.1% DMSO and the inhibitors only .

and for PFDA (ANOVA ($F_{2,4}$ = 9.33, $p < .01$)) viability increased by 10 and 13 percentage points ($p < .05$ and .01, respectively). In contrast, co-incubation with 6 μM memantine significantly decreased viability after PFOA exposure ($p < .05$), whereas 3 μM memantine had no effect. Memantine had no significant effect on viability after PFNA and

PFUnDA exposure. For CPP, concentrations of 0.75, 1.5, 3, 6 and 10 μM significantly increased viability following PFOS exposure (ANOVA ($F_{26,54}$ = 7.08, $p < .001$), Dunnett's post hoc test ($p < .001$)) reaching 86–98% of the 0.1% DMSO control value (only the results for 0.75 and 10 μM are displayed) (Fig. 2C). No effect of co-exposure with 0.75 and
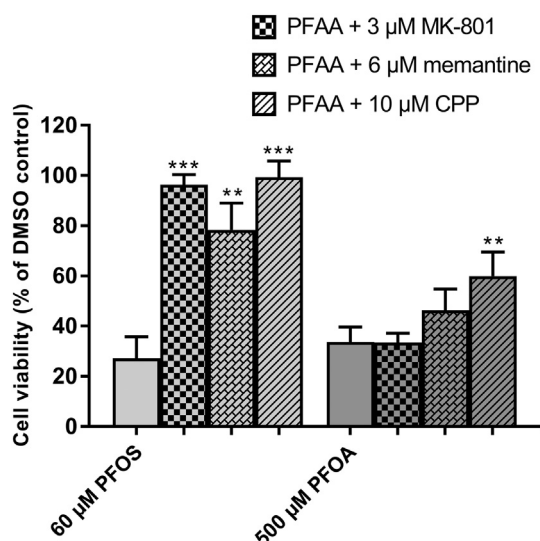
Fig. 3. Neuroprotective effects of ionotropic glutamate receptor antagonists on PFOA and PFOS-induced cytotoxicity at day 14 *in vitro*. Effects on viability after exposure of CGNs for 24 h at day 14 in vitro to PFOS or PFOA alone or together with MK-801, memantine, or CPP were investigated using the MTT assay ($n = 3$ experiments from separate cell isolates). Statistically significant differences are indicated with *, ** and *** representing $p < .05$, $p < .01$ and $p < .001$, respectively. All values are relative to the 0.1% DMSO control in each experiment (defined as 100%).

10 μM CPP was observed for PFHxS, PFOA, PFNA or PFDA. For PFUnDA, very small, but statistically significant increases in viability of 5 and 8 percentage points were observed after co-incubation with 0.75 and 10 μM CPP (ANOVA ($F_{2,5} = 24.1$, $p < .001$), Dunnett's post hoc test ($p < .001$ and .01, respectively)). No effect on viability was observed after co-incubation of CGNs with PFAAs and 10 μM of the AMPA/kainate receptor antagonist NBQX, with the exception of PFUnDA, where a very small statistically significant increase of 3 percentage points was observed ($p < .01$) (Fig. 2D). None of the tested concentrations of the 4 previously mentioned inhibitors had any effect on viability in CGNs unexposed to PFAAs with the exception of 3 μM MK-801, which decreased viability by 13 percentage points as compared to the 0.1% DMSO control (ANOVA ($F_{6,31} = 5.16$, $p < .001$), Dunnett's post hoc test ($p < .001$)) (Fig. 2E).

Involvement of NMDA-Rs in PFOS- and PFOA-induced effects on viability in CGNs expressing mature receptors was also assessed in cells at DIV 14 (Fig. 3). 3 μM MK-801, 6 μM memantine and 10 μM CPP significantly increased cell viability following PFOS exposure by 69, 51 and 72 percentage points, respectively to 96, 78 and 99% of the 0.1% DMSO control (ANOVA ($F_{3,2} = 37.1$, $p < .001$), Dunnett's post hoc test ($p < .001$, .01 and .001, respectively)). For PFOA, viability was increased by 26 percentage points after co-incubation with 10 μM CPP (ANOVA ($F_{3,2} = 18.5$, $p < .01$), Dunnett's post hoc test ($p < .01$)), whereas no statistically significant effects were observed for MK-801 or memantine.

3.2. Effects of PFOS and PFOA on viability in CGNs at different stages of maturation

Exposure of rat CGNs to PFOS and PFOA at DIV 8 and DIV 14, yielded concentration-response curves within the same range of concentrations (10–100 μM and 100–600 μM, respectively) (Fig. 4 A and B). There was a significant difference between the EC_{50} values when the curves for PFOS at DIV 8 (top 104%, Hill-slope − 2.6 and EC_{50} 36 μM) and DIV 14 (top 111%, Hill-slope − 8.3 and EC_{50} 52 μM) were compared (4-parameter model, with bottom constrained to a shared value of 0, $p < .001$). For PFOA the EC_{50} values were not significantly
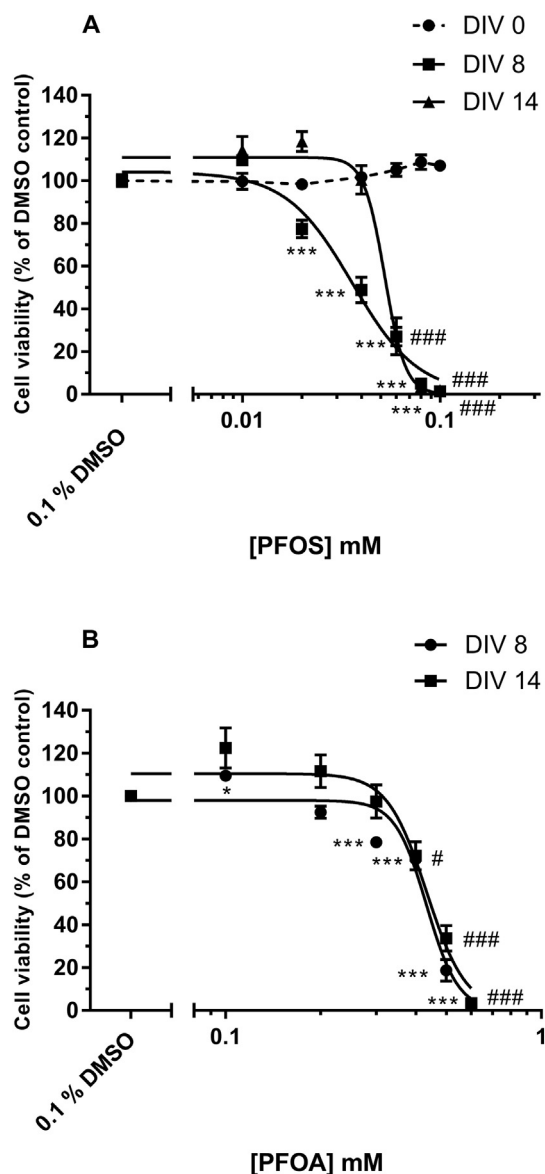

Fig. 4. Effects of PFOS or PFOA exposure on rat cerebellar granule neurons (CGNs) at different stages of maturation. Rat CGNs were exposed to increasing concentrations of A) PFOS at days *in vitro*(DIV) 0, DIV 8 and DIV 14 or B) PFOA at DIV 8 and 14. Viability was assessed after 8 days (exposure DIV 0, n = 3 experiments from separate cell isolates) or 24 h (exposure DIV 8 and 14, n = 5–7 and 3 experiments from separate cell isolates, respectively) exposure. Effects on viability were assessed with the MTT assay. *,** and *** and #,## and ### indicate significant differences from the 0.1% DMSO control of $p < .05$, $p < .01$ and $p < .001$ at DIV 8 and 14, respectively.

different when the curves at DIV 8 (top 98%, Hill-slope − 8.6 and EC_{50} 43 μM) and DIV 14 (top 110%, Hill-slope − 7 and EC_{50} 44 μM) were compared (4-parameter model, with bottom constrained to a shared value of 0). Interestingly, when CGNs were exposed to the same range of PFOS concentrations at time of isolation (DIV 0), and cell viability was assessed at DIV 8, no significant differences from the 0.1% DMSO control could be observed at any of the exposure concentrations. In comparison, exposure of CGNs to PFOS at DIV 8 resulted in significant reductions in cell viability at concentrations of 20 μM and above (ANOVA ($F_{6,28} = 158.3$, $p < .001$)), whereas at DIV 14 reductions were observed from 60 μM and above (ANOVA ($F_{6,14} = 106.1$, $p < .001$)). For PFOA at DIV 8, reductions in viability were observed at concentrations from 300 μM and above (ANOVA ($F_{6,33} = 293.9$, $p < .001$)), whereas at DIV 14 there were significant reductions in
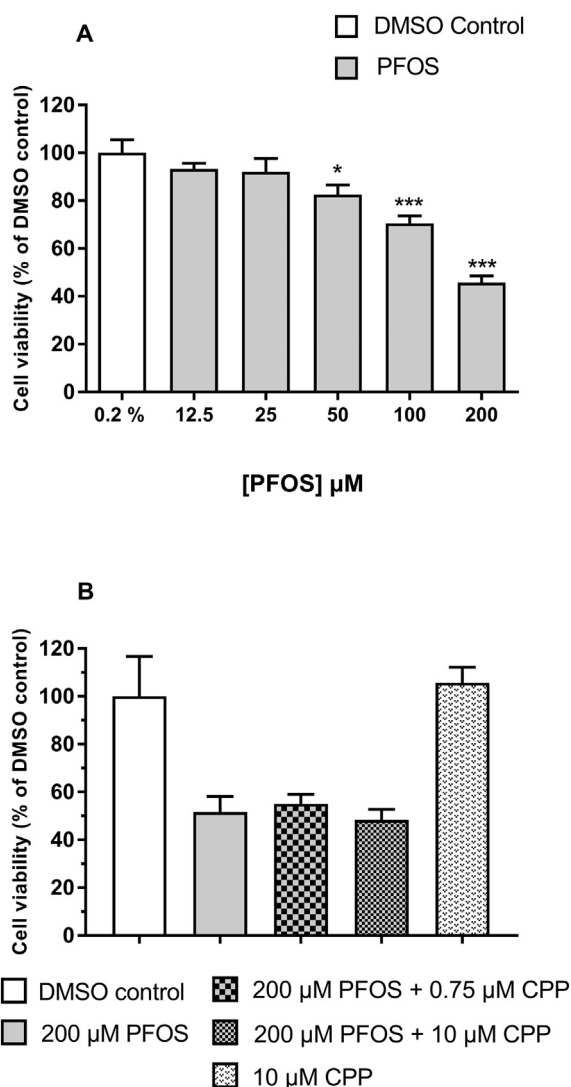
A

B

Fig. 5. Effects of PFOS and inhibitor exposure in PC12 cells. PC12 cells were exposed for 24 h to increasing concentrations of A) PFOS (n = 4 experiments from different culture days) and B) 200 μM PFOS alone and in conjunction with 0.75 or 10 μM CPP, as well as 10 μM CPP only (n = 3 experiments performed on different plates). Effects on viability were assessed with the MTT assay. * and *** indicate statistical significance of p < .05 and p < .001 as compared to the DMSO control.

viability at concentrations of 400 μM or higher (ANOVA ($F_{6,14} = 46.71$, $p < .001$)). At DIV 8 a slight hormetic response was observed for 100 μM PFOA. A similar response was also observed at DIV 14 at the same concentration, although not statistically significant.

3.3. PFOS-induced toxicity in PC12 cells

Effects of PFOS exposure was also repeated for 24 h in PC12 cells lacking the functional expression of NMDA-Rs. Significant reductions in viability were induced at concentrations of 50 μM and above (Fig. 5A) (ANOVA ($F_{5,18} = 23.67$, $p < .001$)). As opposed to complete cyto-toxicity induction in the CGNs after treatment with 100 μM PFOS (Fig. 4A) only a 30 percentage point reduction in viability was observed for the PC12 cells at the same concentration ($p < .05$). After treatment with 200 μM PFOS, viability was reduced by 54 percentage points ($p < .001$). Co-treatment of PC12 cells with 200 μM PFOS and 0.75 or 10 μM CPP, did not result in any improvement in viability as compared to treatment with PFOS alone (Fig. 5B).

3.4. Time-dependent effects on viability of extracellular Ca^{2+} chelation after exposure to PFOS and PFOA

Time-dependent effects on cell viability were assessed using the MTT assay after exposure of CGNs to PFOS (60 μM), PFOS in conjunction with the extracellular Ca^{2+} chelator EGTA (2 mM) or EGTA only for 10, 30 and 60 min, as well as 12 and 24 h (Fig. 6A). Viability-values are expressed as percentage of the 0.1% DMSO control at each time-point (defined as 100%). There was a significant interaction between the effects of time and treatment on viability (2-way ANOVA ($F_{12,60} = 18.06$, $p < .001$)). Simple main effect analysis showed that both time ($F_{4,60} = 29.16$, $p < .001$) and treatment ($F_{3,60} = 149.8$, $p < .001$) had significant effects on viability. PFOS treatment significantly reduced viability after 10, 30 and 60 min by 24, 38 and 46 percentage points, respectively ($p < .01$ for the former, and $p < .001$ for the two latter). Similar effects on viability were observed after treatment with EGTA only with reductions of 34, 47 and 49 percentage points ($p < .001$ for all). After 12 and 24 h treatment PFOS-induced reductions in viability were 60 and 67 percentage points ($p < .001$ for both). When EGTA was applied in conjunction with PFOS this resulted in a significant improvement of viability after 30 and 60 min exposure of 34 percentage points ($p < .001$ for both), as compared to treatment with PFOS alone. After 12 h, co-incubation with PFOS and EGTA re-sulted in a further decrease in viability relative to treatment with PFOS only ($p < .001$), whereas after 24 h, co-treatment decreased viability as compared to treatment with PFOS or EGTA only ($p < .001$ and $p < .01$, respectively). Exposure at the same time-points was also re-peated for PFOA (500 μM) alone or together with EGTA (2 mM) (Fig. 6B), and a significant interaction was found between the effects of the factors time and treatment on viability (2-way ANOVA ($F_{12,60} = 23.81$, $p < .001$)). Both time ($F_{4,60} = 123.6$, $p < .001$) and treatment ($F_{3,60} = 105.5$, $p < .001$) were observed to significantly af-fect viability. Treatment of CGNs with PFOA for 10, 30 or 60 min did not cause significant effects on viability, neither did co-incubation of cells with EGTA and PFOA, this as opposed to treatment with EGTA only. After 12 and 24 h, PFOA-exposure caused decreases in viability of 41 and 91% respectively ($p < .001$ for both).

3.5. Time-dependent effects on viability of intracellular Ca^{2+} chelation after exposure to PFOS and PFOA

Effects on cell viability after co-treatment of CGNs with PFOS (60 μM) or PFOA (500 μM) alone or together with the intracellular Ca^{2+} chelator BAPTA-AM (10 μM), as well as treatment with BAPTA-AM only were assessed after 10 and 60 min, as well as 24 h exposure (Fig. 6C and D). Viability-values are expressed as percentage of the 0.1% DMSO control at each time-point (defined as 100%). For PFOS there was a significant interaction between time and treatment on viability (2-way ANOVA ($F_{6,44} = 5.29$, $p < .001$)). Simple main effect analysis showed that both time ($F_{2,44} = 16.17$, $p < .001$) and treat-ment ($F_{3,44} = 85.79$, $p < .001$) had significant effects on viability. As previously observed, PFOS induced effects on viability after 10 min of exposure. BAPTA-AM did not protect against PFOS-induced effects on viability after 10 or 60 min exposure. After 24 h exposure, co-treatment with PFOS and BAPTA-AM resulted in a further significant decrease in viability of 16 percentage points as compared to treatment with PFOS alone ($p < .01$). Treatment of CGNs with BAPTA-AM significantly de-creased viability after 60 min and 24 h exposure as compared to the 0.2% DMSO control with 25 and 18 percentage points ($p < .001$ and $p < .01$, respectively). For PFOA there was also a significant interac-tion between time and treatment on viability (2-way ANOVA ($F_{6,44} = 33.86$, $p < .001$)), and simple main effect analysis showed that both time ($F_{2,44} = 98.11$, $p < .001$) and treatment ($F_{3,44} = 77.33$, $p < .001$) had significant effects on viability. No significant effects of PFOA were observed after 10 or 60 min exposure. After 24 h exposure there was no significant difference in viability after treatment with
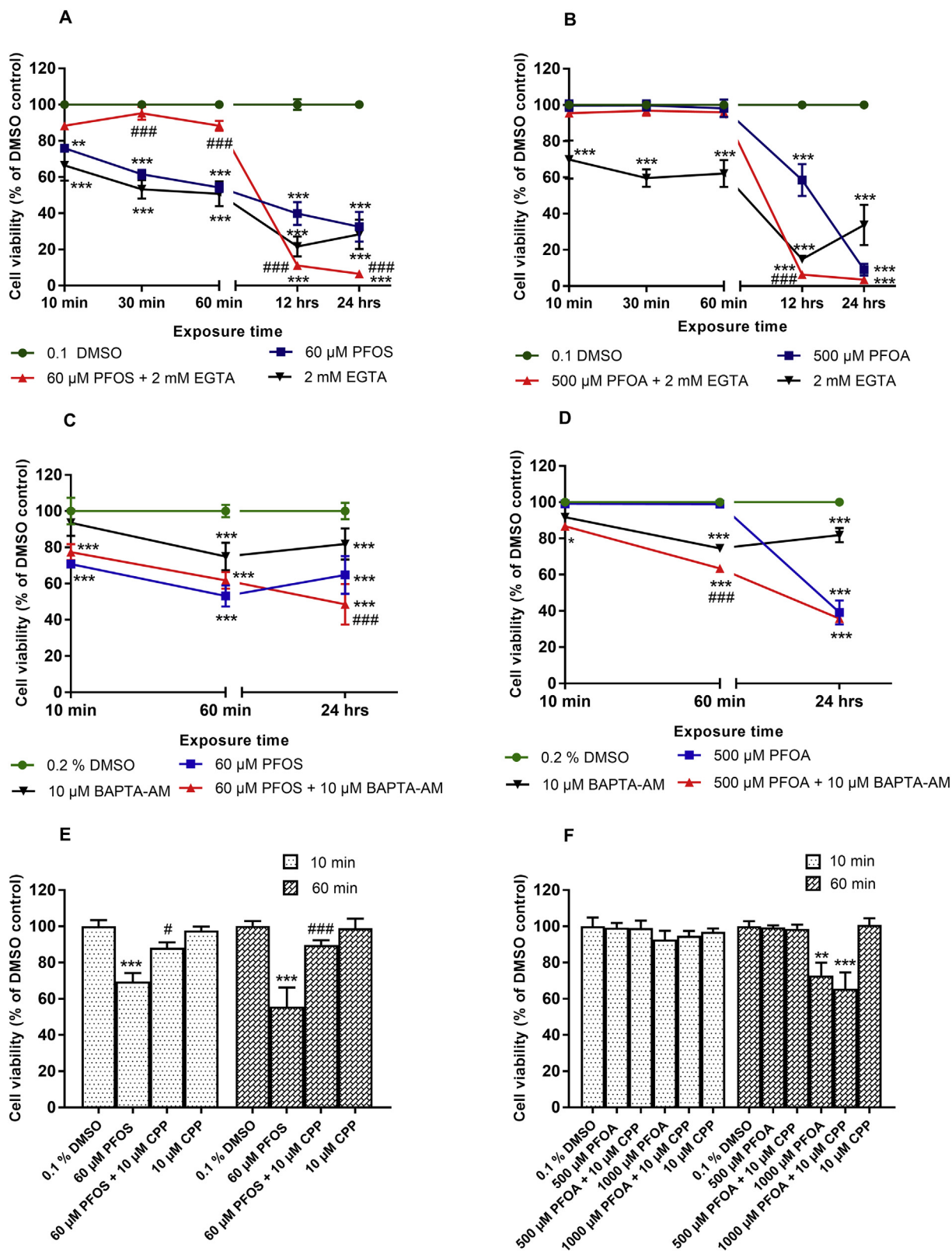
Fig. 6. Time-dependent changes in viability of cerebellar granule neurons (CGNs) after exposure to PFOS and PFOA, alone and in conjunction with EGTA, BAPTA-AM or CPP. CGNs were exposed to PFOS and PFOA alone or together with A) and B) EGTA for 10, 30 and 60 min as well as 12 and 24 h (n = 4). C) and D) BAPTA-AM for 10 and 60 min as well as 24 h (n = 4–6). E) and F) CPP for 10 and 60 min (n = 4–5 and n = 3–5). In each experiment the inhibitor alone as well as a relevant DMSO control were also included. Effects on viability were assessed with the MTT assay, and expressed as % of the DMSO control at each time-point. Statistically significant differences from the DMSO control are indicated with ** and *** representing $p < .01$ and $p < .001$. Significant differences between PFOS or PFOA alone or together with EGTA/BAPTA-AM or CPP are indicated with # or ### for $p < .05$ and $p < .001$, respectively.

PFOA or PFOA in conjunction with BAPTA-AM.

3.6. Effects of CPP on time-dependent changes in viability after PFOS and PFOA exposure

In addition to the experiments conducted with the NMDA-R antagonist CPP after 24 h exposure (Fig. 2C), effects on viability after co-treatment of CGNs with PFOS (60 μM) or PFOA (500 μM and 1000 μM) alone or together with CPP (10 μM) was assessed after 10 and 60 min exposure (Fig. 6E and F). Effects of exposure to CPP only, was also examined. Viability-values are expressed as percentage of the 0.1% DMSO control at each time-point (defined as 100%). For PFOS there was no significant interaction between the effects of time and treatment on viability (2-way ANOVA). Simple main effect analysis further showed no effect of time, but a significant effect of treatment ($F_{3,20} = 28.16$, $p < .001$) on viability. After both 10 and 60 min CPP significantly increased viability after PFOS exposure from 70 and 56% to 88 and 90%, respectively ($p < .05$ and $p < .001$). CPP only had no significant effects on viability. For PFOA there was a significant interaction between time and treatment on viability (2-way ANOVA ($F_{5,32} = 4.87$, $p < .01$)), and simple main effect analysis showed that both time ($F_{1,32} = 9.67$, $p < .01$) and treatment ($F_{5,32} = 8.90$, $p < .001$) had significant effects on viability. None of the applied treatments had any effect after 10 min of exposure, whereas after 60 min exposure 1000 μM PFOA significantly reduced viability with 27 percentage points to 73% of the DMSO control ($p < .01$). Co-incubation with 1000 μM PFOA and 10 μM CPP did not result in any significant alterations in viability as compared to 1000 μM PFOA only.

3.7. Effects of PFOS and PFOA exposure on cytosolic Ca^{2+} concentration

$[Ca^{2+}]_i$ was measured after exposure of CGNs to sBME ($-$ FBS) alone or to 60, 100 and 300 μM PFOS or PFOA, at time-point 0 (before treatment) and after 30 and 60 min exposure. $[Ca^{2+}]_i$ was expressed relative to the measurements at time-point 0, set to 1 (Fig. 7A and B). Due to lack of effects after exposure to PFOA, a very high concentration of PFOS and PFOA (1000 μM) was also included. After exposure to 1000 μM PFOS, cells were observed to burst and die under the microscope, these results were therefore excluded from graphs and statistical analysis. For PFOS there was no significant interaction between effects of time and concentration on $[Ca^{2+}]_i$ (2-way ANOVA). Simple main effect analysis showed that both time ($F_{2,48} = 38$, $p < .001$), and concentration ($F_{3,48} = 6.16$, $p < .01$) had significant effects on $[Ca^{2+}]_i$. When exposure to 300 μM PFOS was compared with exposure to sBME ($-$ FBS) only, after both 30 and 60 min $[Ca^{2+}]_i$ was significantly increased ($p < .01$). Exposure to 60 and 100 μM PFOS showed no significant effect. Results were, however, close to significance after 30 min ($p = .05$, for both). When compared to time-point 0, both 30 and 60 min exposure to all three concentrations of PFOS caused significant increases in $[Ca^{2+}]_i$. When exposure to sBME ($-$ FBS) only was compared to time 0 there were no significant increases in $[Ca^{2+}]_i$ observed after 30 and 60 min.

Also for PFOA there was no significant interaction between effects of time and concentration on $[Ca^{2+}]_i$ (2-way ANOVA). Further, time had a significant effect ($F_{2,51} = 29.58$, $p < .001$), whereas no significant effect on $[Ca^{2+}]_i$ was induced by exposure. As such there was no difference between cells treated with sBME ($-$ FBS) only or any concentration of PFOA at any time-point. After 1 h exposure a significant increase in $[Ca^{2+}]_i$ was observed as compared to time-point 0 for all the PFOA concentrations, but such an increase was also observed for treatment with sBME ($-$ FBS) alone ($p < .05$ or below).

3.8. Effects of PFOS and PFOA exposure in conjunction with MK-801 on cytosolic Ca^{2+} concentration

To assess the involvement of extracellular Ca^{2+} influx via the NMDA-R in PFOS or PFOA-induced increases in $[Ca^{2+}]_i$, CGNs were exposed to 300 μM PFOS or PFOA, alone or in combination with 3 μM of the NMDA-R antagonist MK-801 (Fig. 7C and D). Cells were also exposed to MK-801 + sBME ($-$ FBS) or BME ($-$ FBS) only. For PFOS, there was a significant interaction between the effects of time and treatment on $[Ca^{2+}]_i$ (2-way ANOVA ($F_{6,72} = 8.19$, $p < .001$)). Further, both time ($F_{2,72} = 28.47$, $p < .001$) and treatment ($F_{3,72} = 31.95$, $p < .001$) had significant effects on $[Ca^{2+}]_i$. Again, 300 μM PFOS significantly increased $[Ca^{2+}]_i$ as compared to treatment with sBME ($-$ FBS) after 30 and 60 min exposure, and the increases after PFOS exposure were also significantly different as compared to time point-0 ($p < .001$ for all). When MK-801 was added to the cells 5 min prior to exposure to PFOS, the increase in $[Ca^{2+}]_i$ was completely abolished, as shown by a flat line after 30 or 60 min exposure (Fig. 7C), and $[Ca^{2+}]_i$ was significantly different as compared to after PFOS only treatment at 30 and 60 min of exposure ($p < .001$). Treatment with MK-801 + sBME ($-$ FBS) as compared to sBME ($-$ FBS) only did not induce significant differences in $[Ca^{2+}]_i$, as illustrated by the parallel lines. For PFOA there was no significant interaction between effects of time and exposure on $[Ca^{2+}]_i$ (2-way ANOVA). Further, time had a significant effect ($F_{2,66} = 53.28$, $p < .001$), whereas no significant effect was induced by exposure on $[Ca^{2+}]_i$, also illustrated by the parallel lines in Fig. 7D.

4. Discussion

In the present study we have shown that three different antagonists of the NMDA-R protected against PFOS-induced effects on cell viability after 24 h exposure in rat CGNs at DIV 8. This was also confirmed in CGNs exposed at DIV 14. Exposure of CGNs to PFOS and PFOA at DIV 8 and 14, yielded viability concentration-response curves within the same concentration ranges at the two time-points, whereas no effect on viability was observed when cells were exposed to PFOS at DIV 0. When PC12 cells were exposed to high PFOS concentrations (up to 200 μM), partial, but not complete reduction in viability was induced, and these reductions in viability were not blocked by co-treatment with CPP. Treatment of CGNs with the extracellular Ca^{2+} chelator EGTA significantly protected against PFOS-induced reductions in viability after 30 and 60 min exposure, whereas no such effect could be observed for the intracellular Ca^{2+} chelator BAPTA-AM. CPP also protected against PFOS-induced reductions in viability after 10 and 60 min exposure. PFOS exposure further caused significant increases in cytosolic levels of free Ca^{2+}, after 30 and 60 min exposure, which was blocked by addition of the NMDA-R antagonist MK-801, prior to toxicant application.

Significant improvement in viability was observed after co-treatment of cells at DIV 8 with the sulfonated PFAA PFOS and either of the uncompetitive NMDA-R open channel blockers MK-801 and memantine (Ates-Alagoz and Adejare, 2013; Chen and Lipton, 1997; Chen et al., 1992; Cottone et al., 2013; Frankiewicz et al., 1996) or the competitive antagonist CPP (Fritz et al., 1996) (Fig. 2A, B and C). Like Mg^{2+}, MK-801 and memantine bind within the channel of the NMDA-R (Chen and Lipton, 1997; Frankiewicz et al., 1996; Volbracht et al., 2006), preventing Ca^{2+} influx. Memantine has a faster kinetic binding profile and more rapid blocking and unblocking rate (Chen et al., 1992), as well as a greater voltage dependence than MK-801 (Frankiewicz et al., 1996), which may potentially explain the somewhat higher protective effect of MK-801 compared to memantine against PFOS-induced excitotoxicity observed in the present study. CPP on the other hand, acts as a competitive antagonist at the orthosteric glutamate binding site of the receptor (Fritz et al., 1996), blocking the activation of the receptor by prevention of glutamate binding. Significant protection against effects on cell viability with three different antagonists of the NMDA-R strongly suggest an involvement of this receptor in PFOS-induced cytotoxicity.

Some protection against effects on viability was also observed after co-treatment of CGNs with another sulfonated PFAA, the two carbon
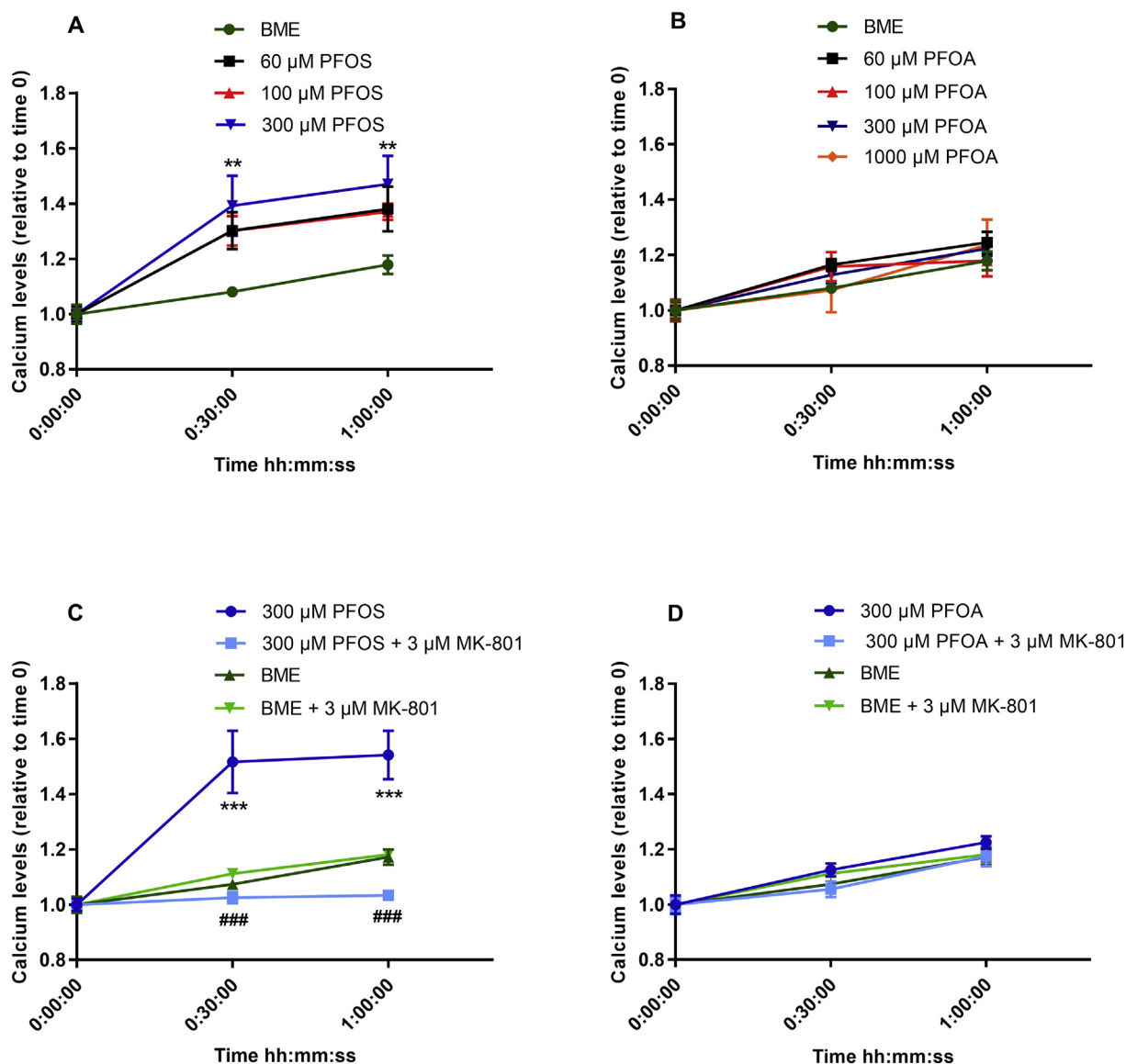
Fig. 7. Ca^{2+} levels in cerebellar granule neurons (CGNs) after exposure to BME, PFOS or PFOA, alone or together with MK-801. CGNs were exposed to sBME (− FBS), or 60, 100, 300 or 1000 μM of A) PFOS or B) PFOA and cytosolic Ca^{2+} ($[Ca^{2+}]_i$) measured at time-point 0, as well as after 30 min and 1 h exposure using Fura-2 Ca^{2+} imaging (n = 4–5). $[Ca^{2+}]_i$ levels are expressed relative to the measurements at time-point 0, set to 1. The results for 1000 μM PFOS are not displayed. $[Ca^{2+}]_i$ was also measured after exposure of CGNs to 300 μM of C) PFOS or D) PFOA, alone or together with 3 μM MK-801 (n = 6–8). Cells were additionally exposed to sBME (− FBS) or 3 μM MK-801 in sBME (− FBS). Statistically significant differences between $[Ca^{2+}]_i$ in CGNs treated with PFOS and sBME (− FBS) are indicated with ** and *** representing p < .01 and p < .001, respectively. Significant differences between PFOS alone or together with MK-801 are indicated with ### for p < .001. For ease sBME (− FBS) is written as BME within the figures.

atom shorter PFHxS, and the blockers MK-801 and memantine (Fig. 2 A and B). Protective effects of MK-801 against PFHxS-induced apoptosis as well as PFHxS-induced increases in intracellular Ca^{2+} in CGNs was also reported in a recent study by Lee et al. (2016). Interestingly, in the present study, no protection was afforded by the antagonist CPP against PFHxS-induced effects on viability (Fig. 2C). In Berntsen et al. (2017) we observed that PFHxS-induced effects on viability in CGNs had a slow onset (between 18 and 24 h) when compared to equipotent concentrations of PFOS (inducing cytotoxicity within 60 min). This suggests that whereas PFOS induces rapid excitotoxicity, and Ca^{2+} influx via glutamate-induced NMDA receptor activation, PFHxS at equipotent concentrations (as examined after 24 h exposure), induces cell death in a slower and perhaps more apoptotic-like manner that to some extent involves Ca^{2+} influx via the NMDA-R. After 24 h exposure to the four carboxylated PFAAs; PFOA, PFNA, PFDA and PFUnDA there was no large protective effect observed after co-treatment with MK-801,

memantine or CPP (Fig. 2A, B and C). For PFOA a significant reduction in viability was observed after exposure in conjunction with MK-801 and memantine, also observed for PFNA and memantine (Fig. 2A and B). MK-801 also had a negative effect on viability in CGNs unexposed to PFAAs (Fig. 2E). These negative effects on viability may be explained by the fact that CGNs in culture requires some stimulation of the NMDA-Rs for survival. CGNs are grown under partly depolarising conditions at high potassium concentrations (25 mM), believed to mimic activation by input from mossy fibres (Gallo et al., 1987; Vallano et al., 1996). Blockage of the NMDA-R channel may thus have negative effects on viability in both exposed and unexposed neurons. Co-incubation of CGNs with PFAAs and the antagonist NBQX, which acts on the ionotropic glutamate receptors AMPA and kainate, did not significantly affect viability (with the exception of PFUnDA, where the biological relevance is questionable) (Fig. 2D). The absence of effects using AMPA/kainate-R blockers likely indicates that the observed PFOS-

induced effects were mainly induced via NMDA-R activation.

The large protective effects of MK-801, memantine and CPP, against PFOS-induced toxicity at DIV 8, were reproducible in neurons exposed at DIV 14, where they were even more pronounced (Fig. 3). Interestingly, at this stage no negative effects on viability were observed after co-treatment of cells with PFOA and MK-801 or memantine, and a slight protective effect was also observed after co-treatment with CPP. These differences could potentially be explained by changes in NMDA-R subunit composition, occurring during the maturation of the neuronal cultures. It has been previously observed that GluN2B subunits in cultures of CGNs are gradually replaced by GluN2A and GluN2C subunits as culture days in vitro (DIV) increase from 0 to 14 (Cebers et al., 2001; Vallano et al., 1996). Another finding in the present study, which could potentially be related to changes in GluN2 subunit expression, could be the lack of toxicity observed when CGNs were exposed to increasing concentrations of PFOS at DIV 0 (Fig. 4A). Cells at this stage of maturation are predominantly expressing NMDA-R containing GluN2B subunits. In previous studies lack of toxicity to glutamate from serum or nutrient mediums has been observed in newly isolated CGNs from rats, and is likely due to the undifferentiated state of these neurons at the time of isolation (Schramm et al., 1990). Another possible explanation for the observed lack of toxicity is that PFOS may bind to serum proteins in the medium, as medium with 10% FBS was used due to growth requirements when plating at DIV 0, whereas no serum was used when cells were exposed at DIV 8 and 14. PFAAs do seem to have high affinity for serum proteins, and proteins in general. On the other hand, in PC12 cells, a reduction in viability of 25% was observed after exposure to 100 μM PFOS, despite the presence of 10% FBS and 5% horse serum (Fig. 5A), a concentration not affecting viability in CGNs at DIV 0, but inducing complete toxicity at DIV 8 exposure (Fig. 4A). So binding to serum proteins is not likely to be the only explanation for the lack of an effect observed after exposure of CGNs at DIV 0. Further studies examining the effects of PFOS in cells expressing immature receptors are necessary to clarify this point.

When undifferentiated PC12 cells were exposed to concentrations of PFOS within the same concentration-range as the CGNs, the induced toxicity was notably lower. Not even after application of a concentration 2 times that required to induce 100% toxicity in the CGNs, was full toxicity induced (Fig. 5A). In concordance with our results, around 40% reduction in viability in PC12 cells after 24 h exposure to 250 μM PFOS was also reported in a recent study by Li et al. (2017). A possible explanation for the lower PFOS-induced toxicity in PC12 cells may be their reported lack of expression of functional NMDA-R (Edwards et al., 2007), or as discussed previously the presence of serum in the medium. As opposed to the protective effect of CPP treatment observed in rat CGNs against PFOS-induced effects on viability (Fig. 2C and 3), no protection was afforded by CPP in the PC12 cells (Fig. 5B). Li et al. (2017) found an increase in the production of reactive oxygen species (ROS) in PC12 cells, after PFOS exposure, which was reduced by co-treatment with taurine treatment. In the present study we also found that a mixture of the anti-oxidants vitamin E and C protected against PFOS-induced effects on viability (results not shown).

Due to previous observations that PFOS induced most of its effects on viability within 60 min (Berntsen et al., 2017), we investigated how the extracellular Ca^{2+} chelator EGTA, the intracellular Ca^{2+} chelator BAPTA-AM, and the competitive NMDA-R antagonist CPP affected viability within this time period. Both application of EGTA and CPP significantly improved viability after PFOS exposure within the 60 first min (Fig. 6A and E), suggesting that the PFOS-induced effects on viability are dependent on extracellular Ca^{2+} influx via the NMDA receptor. No significant protection was induced by co-treatment with the intracellular Ca^{2+} chelator BAPTA-AM (Fig. 6C). The significant effects observed using NMDA-R antagonists and extracellular calcium chelators and lack of effects using intracellular calcium chelators are in concordance with previously published literature on excitotoxicity. Rapid excitotoxicity is not just dependent on elevated intracellular

calcium, but also on movement of Ca^{2+} through the NMDA-R channel, and activation of downstream toxic pathways. Entry of excess Ca^{2+} through the receptor channel would elevate local calcium transients above baseline values resulting in binding of scaffolding proteins such as postsynaptic density-95 (PSD-95), which links the NMDA-R to intracellular signaling molecules such as e.g. NO that mediate the toxic effects (Sattler et al., 1999). As a result, chelation of extracellular calcium or use of NMDA-R antagonists would reduce Ca^{2+} flux and act in a neuroprotective manner, whereas chelation of intracellular calcium would not reduce flux, but might even increase it resulting in increased toxicity when using higher concentrations of BAPTA-AM. In accordance with our previous experiments, PFOA in contrast to PFOS at a concentration of 500 μM did not induce any observable toxicity during 1 h exposure, and thus no effects were observed after co-treatment with inhibitors (Fig. 6B, D and F). In an attempt to induce toxicity, we therefore also treated the CGNs with a high concentration of PFOA (1000 μM) for 10 and 60 min. At 60 min, some degree of toxicity was then observed (Fig. 6F), however, no protection was afforded by co-treatment with CPP, indicating a different mechanism of action for PFOA as compared to PFOS.

When we further examined how $[Ca^{2+}]_i$ in CGNs was affected by PFOS, we found that it was significantly increased after 30 and 60 min exposure to 300 μM PFOS as compared to control cells (Fig. 7A). Also, concentrations of 60 and 100 μM PFOS increased Ca^{2+} levels, although not in a statistically significant way (borderline significance after 30 min). Pre-treatment with MK-801 in subsequent experiments completely abolished the PFOS-induced increases in $[Ca^{2+}]_i$, indicating that the increases were mediated through influx via the NMDA-R (Fig. 7C). For PFOA, no increases in $[Ca^{2+}]_i$ were observed when concentrations up to 300 μM were applied, which could be expected due to the previously observed lack of effects on viability prior to 12 h (Berntsen et al., 2017). Also the application of a higher concentration of PFOA (1000 μM) failed to induce any increase in $[Ca^{2+}]_i$, supporting a different mechanism of action not involving Ca^{2+} influx for the above mentioned toxicity induced after treatment of CGNs with this high concentration. Although no statistically significant changes in $[Ca^{2+}]_i$ could be detected after exposure to the lower PFOS concentrations, this does not preclude the possibility that intracellular release mechanisms could be compromised at lower PFOS concentrations leading to neuronal injury rather than neuronal cell death. Intracellular mechanisms of Ca^{2+} release were not investigated in the present study, but represent interesting future studies.

The observed increases in $[Ca^{2+}]_i$ in the present study may be linked to findings reported by others after exposure of various neuronal cell models to PFOS or other sulfonated PFAAs such as PFHxS. As discussed by Lee et al. (2016) overstimulation of the NMDA-R may lead to excessive Ca^{2+} influx, which causes membrane depolarisation and activation of L-type voltage-dependent calcium channels (L-VDCCs), which may cause further increase in $[Ca^{2+}]_i$. The involvement of both the NMDA-R and L-VDCCs was confirmed in PFHxS-induced increases in $[Ca^{2+}]_i$ in the experiments by Lee et al. (2016) using rat CGNs. PFOS-induced Ca^{2+} influx via L-VDCCs has also been observed in studies in primary hippocampal neurons from rat (Liao et al., 2008). In addition to influx of Ca^{2+} from the extracellular environment, release of Ca^{2+} from intracellular stores has been reported after PFOS exposure in rat hippocampal neurons by Liu et al. (2011) where the liberation was mainly occurring through inositol 1,4,5-triphoshate receptors (IP₃Rs) and ryanodine receptors (RyRs). As Ca^{2+} acts as a second messenger it may potentially activate several downstream signaling pathways and events. In Lee et al. (2016) PFHxS-induced increases in $[Ca^{2+}]i$ was found to be linked to the induction of apoptosis via the mitogen-activated protein kinase (MAPK) extracellular signal-regulated kinase (ERK) 1/2 pathway. Apoptosis induction in CGNs through ERK 1/2 activation was also observed in the studies by Lee et al. (2013) and Lee et al. (2014) in CGNs after exposure to PFOS and PFHxS, respectively. Whereas the activation of ERK after PFOS exposure was found to occur

through a ROS-dependent activation of protein kinase C (PKC) (Lee et al., 2012; Lee et al., 2013), experiments using PFHxS indicated that ROS production here was rather a downstream target and not an upstream regulator of ERK 1/2 activation (Lee et al., 2014). Despite these previous reports and mechanisms discussed, chelation of $[Ca^{2+}]_i$ in the present study did not affect toxicity, indicating that any contribution via other Ca^{2+} channels is secondary to that of the NMDA-R.

PFOS was listed as a persistent chemical under the Stockholm Convention on Persistent Organic Pollutants in 2009 (UNEP, 2010), but is still in use in China (Fu et al., 2016). The concentration of PFOS used in the present study is higher than levels in the general population, and would be more relevant for an occupational setting. A recent Chinese study found levels of PFOS up to 118,000 ng/ml (236 μM) in serum from occupationally exposed workers (Fu et al., 2016). Assuming a concentration in the brain as 25% of the concentration in serum based on Maestri et al. (2006), this corresponds to a concentration of 60 μM. In the present study we saw that concentrations of 60 μM significantly affected cell viability and increased cytosolic Ca^{2+} (although not statistically significant).

5. Conclusion

In conclusion, excitotoxicity induction by PFOS in CGNs is likely to happen mainly through over-activation of the NMDA-R and excess influx of Ca^{2+}. This was confirmed by protective effects using competitive and uncompetitive NMDA-R antagonists and an absence of protective effects for the AMPA/Kainate-R antagonist NBQX. The channel blockers memantine and MK-801 also showed some effects against PFHxS-induced reductions in viability. No significant involvement of the NMDA-R in PFCA-induced effects on viability could be observed in the present study, perhaps with the exception of PFOA in mature CGNs. PFOS-induced effects occurred within a few hours, at concentrations that may be relevant in an occupational setting.

Conflict of interest statement

The authors declare that there are no conflicts of interest.

Acknowledgements

References

Ahrens, L., Siebert, U., Ebinghaus, R., 2009. Total body burden and tissue distribution of polyfluorinated compounds in harbor seals (Phoca vitulina) from the German Bight. Mar. Pollut. Bull. 58 (4), 520–525.

Akazawa, C., Shigemoto, R., Bessho, Y., Nakanishi, S., Mizuno, N., 1994. Differential expression of five N-methyl-D-aspartate receptor subunit mRNAs in the cerebellum of developing and adult rats. J. Comp. Neurol. 347 (1), 150–160.

Ates-Alagoz, Z., Adejare, A., 2013. NMDA Receptor Antagonists for Treatment of Depression. Pharmaceuticals (Basel) 6 (4), 480–499.

Berntsen, H.F., Wigestrand, M.B., Bogen, I.L., Fonnum, F., Walaas, S.I., Moldes-Anaya, A., 2013. Mechanisms of penitrem-induced cerebellar granule neuron death in vitro: possible involvement of GABAA receptors and oxidative processes. Neurotoxicology 35, 129–136.

Berntsen, H.F., Bjorklund, C.G., Audinot, J.N., Hofer, T., Verhaegen, S., Lentzen, E., Gutleb, A.C., Ropstad, E., 2017. Time-dependent effects of perfluorinated compounds on viability in cerebellar granule neurons: Dependence on carbon chain length and functional group attached. Neurotoxicology 63, 70–83.

Buck, R.C., Franklin, J., Berger, U., Conder, J.M., Cousins, I.T., de Voogt, P., Jensen, A.A., Kannan, K., Mabury, S.A., van Leeuwen, S.P., 2011. Perfluoroalkyl and polyfluoroalkyl substances in the environment: terminology, classification, and origins. Integr. Environ. Assess. Manag. 7 (4), 513–541.

Buckner, R.L., 2013. The cerebellum and cognitive function: 25 years of insight from anatomy and neuroimaging. Neuron 80 (3), 807–815.

Cebers, G., Cebere, A., Kovacs, A.D., Hogberg, H., Moreira, T., Liljequist, S., 2001. Increased ambient glutamate concentration alters the expression of NMDA receptor subunits in cerebellar granule neurons. Neurochem. Int. 39 (2), 151–160.

Chen, H.S., Lipton, S.A., 1997. Mechanism of memantine block of NMDA-activated channels in rat retinal ganglion cells: uncompetitive antagonism. J. Physiol. 499,

27–46 Pt 1.

Chen, H.S., Pellegrini, J.W., Aggarwal, S.K., Lei, S.Z., Warach, S., Jensen, F.E., Lipton, S.A., 1992. Open-channel block of N-methyl-D-aspartate (NMDA) responses by memantine: therapeutic advantage against NMDA receptor-mediated neurotoxicity. J. Neurosci. 12 (11), 4427–4436.

Chen, J., Das, S.R., La Du, J., Corvi, M.M., Bai, C., Chen, Y., Liu, X., Zhu, G., Tanguay, R.L., Dong, Q., Huang, C., 2013. Chronic PFOS exposures induce life stage-specific behavioral deficits in adult zebrafish and produce malformation and behavioral deficits in F1 offspring. Environ. Toxicol. Chem. 32 (1), 201–206.

Cottone, P., Iemolo, A., Narayan, A.R., Kwak, J., Momaney, D., Sabino, V., 2013. The uncompetitive NMDA receptor antagonists ketamine and memantine preferentially increase the choice for a small, immediate reward in low-impulsive rats. Psychopharmacology 226 (1), 127–138.

de Luca, A., Weller, M., Fontana, A., 1996. TGF-beta-induced apoptosis of cerebellar granule neurons is prevented by depolarization. J. Neurosci. 16 (13), 4174–4185.

Edwards, M.A., Loxley, R.A., Williams, A.J., Connor, M., Phillips, J.K., 2007. Lack of functional expression of NMDA receptors in PC12 cells. Neurotoxicology 28 (4), 876–885.

Eggers Pedersen, K., Basu, N., Letcher, R., Greaves, A.K., Sonne, C., Dietz, R., Styrishave, B., 2015. Brain region-specific perfluoroalkylated sulfonate (PFSA) and carboxylic acid (PFCA) accumulation and neurochemical biomarker responses in East Greenland polar bears (Ursus maritimus). Environ. Res. 138, 22–31.

Feng, B., Tse, H.W., Skifter, D.A., Morley, R., Jane, D.E., Monaghan, D.T., 2004. Structure-activity analysis of a novel NR2C/NR2D-preferring NMDA receptor antagonist: 1-(phenanthrene-2-carbonyl) piperazine-2,3-dicarboxylic acid. Br. J. Pharmacol. 141 (3), 508–516.

Fonnum, F., Lock, E.A., 2004. The contributions of excitotoxicity, glutathione depletion and DNA repair in chemically induced injury to neurones: exemplified with toxic effects on cerebellar granule cells. J. Neurochem. 88 (3), 513–531.

Frankiewicz, T., Potier, B., Bashir, Z.I., Collingridge, G.L., Parsons, C.G., 1996. Effects of memantine and MK-801 on NMDA-induced currents in cultured neurones and on synaptic transmission and LTP in area CA1 of rat hippocampal slices. Br. J. Pharmacol. 117 (4), 689–697.

Fritz, K.I., Groenendaal, F., McGowan, J.E., Mishra, O.P., Delivoria-Papadopoulos, M., 1996. Effect of cerebral hypoxia on NMDA receptor binding characteristics after treatment with 3-(2-carboxypiperazin-4-yl)propyl-1-phosphonic acid (CPP) in newborn piglets. Brain Res. 729 (1), 66–74.

Fu, J., Gao, Y., Cui, L., Wang, T., Liang, Y., Qu, G., Yuan, B., Wang, Y., Zhang, A., Jiang, G., 2016. Occurrence, temporal trends, and half-lives of perfluoroalkyl acids (PFAAs) in occupational workers in China. Sci. Rep. 6, 38039.

Gallo, V., Ciotti, M.T., Coletti, A., Aloisi, F., Levi, G., 1982. Selective release of glutamate from cerebellar granule cells differentiating in culture. Proc. Natl. Acad. Sci. U. S. A. 79 (24), 7919–7923.

Gallo, V., Kingsbury, A., Balazs, R., Jorgensen, O.S., 1987. The role of depolarization in the survival and differentiation of cerebellar granule cells in culture. J. Neurosci. 7 (7), 2203–2213.

Greaves, A.K., Letcher, R.J., Sonne, C., Dietz, R., 2013. Brain region distribution and patterns of bioaccumulative perfluoroalkyl carboxylates and sulfonates in East Greenland polar bears (Ursus maritimus). Environ. Toxicol. Chem. 32 (3), 713–722.

Haug, L.S., Salihovic, S., Jogsten, I.E., Thomsen, C., van Bavel, B., Lindstrom, G., Becher, G., 2010. Levels in food and beverages and daily intake of perfluorinated compounds in Norway. Chemosphere 80 (10), 1137–1143.

Holzer, J., Goen, T., Rauchfuss, K., Kraft, M., Angerer, J., Kleeschulte, P., Wilhelm, M., 2009. One-year follow-up of perfluorinated compounds in plasma of German residents from Arnsberg formerly exposed to PFOA-contaminated drinking water. Int. J. Hyg. Environ. Health 212 (5), 499–504.

Hoyer, B.B., Ramlau-Hansen, C.H., Obel, C., Pedersen, H.S., Hernik, A., Ogniev, V., Jonsson, B.A., Lindh, C.H., Rylander, L., Rignell-Hydbom, A., Bonde, J.P., Toft, G., 2015. Pregnancy serum concentrations of perfluorinated alkyl substances and off-spring behaviour and motor development at age 5-9 years–a prospective study. Environ. Health 14, 2.

Iacobucci, G.J., Popescu, G.K., 2018. Kinetic models for activation and modulation of NMDA receptor subtypes. Curr. Opinion in Physiol. 2, 114–122.

Johansson, N., Fredriksson, A., Eriksson, P., 2008. Neonatal exposure to perfluorooctane sulfonate (PFOS) and perfluorooctanoic acid (PFOA) causes neurobehavioural defects in adult mice. Neurotoxicology 29 (1), 160–169.

Kew, J.N., Kemp, J.A., 2005. Ionotropic and metabotropic glutamate receptor structure and pharmacology. Psychopharmacology 179 (1), 4–29.

Kotthoff, M., Muller, J., Jurling, H., Schlummer, M., Fiedler, D., 2015. Perfluoroalkyl and polyfluoroalkyl substances in consumer products. Environ. Sci. Pollut. Res. Int. 22 (19), 14546–14559.

Kramer, D., Minichiello, L., 2010. Cell culture of primary cerebellar granule cells. Methods Mol. Biol. 633, 233–239.

Lee, H.G., Lee, Y.J., Yang, J.H., 2012. Perfluorooctane sulfonate induces apoptosis of cerebellar granule cells via a ROS-dependent protein kinase C signaling pathway. Neurotoxicology 33 (3), 314–320.

Lee, Y.J., Lee, H.G., Yang, J.H., 2013. Perfluorooctane sulfonate-induced apoptosis of cerebellar granule cells is mediated by ERK 1/2 pathway. Chemosphere 90 (5), 1597–1602.

Lee, Y.J., Choi, S.Y., Yang, J.H., 2014. PFHxS induces apoptosis of neuronal cells via ERK1/2-mediated pathway. Chemosphere 94, 121–127.

Lee, E., Choi, S.Y., Yang, J.H., Lee, Y.J., 2016. Preventive effects of imperatorin on perfluorohexanesulfonate-induced neuronal apoptosis via inhibition of intracellular calcium-mediated ERK pathway. Korean J. Physiol. Pharmacol. 20 (4), 399–406.

Li, C.Y., Chin, T.Y., Chueh, S.H., 2004. Rat cerebellar granule cells are protected from glutamate-induced excitotoxicity by S-nitrosoglutathione but not glutathione. Am. J.

Phys. Cell Phys. 286 (4), C893–C904.

Li, C., Liu, X., Liu, Q., Li, S., Li, Y., Hu, H., Shao, J., 2017. Protection of Taurine against PFOS-Induced Neurotoxicity in PC12 Cells. Adv. Exp. Med. Biol. 975, 907–916.

Liao, C.Y., Li, X.Y., Wu, B., Duan, S., Jiang, G.B., 2008. Acute enhancement of synaptic transmission and chronic inhibition of synaptogenesis induced by perfluorooctane sulfonate through mediation of voltage-dependent calcium channel. Environ. Sci. Technol. 42 (14), 5335–5341.

Liu, X., Jin, Y., Liu, W., Wang, F., Hao, S., 2011. Possible mechanism of perfluorooctane sulfonate and perfluorooctanoate on the release of calcium ion from calcium stores in primary cultures of rat hippocampal neurons. Toxicol. in Vitro 25 (7), 1294–1301.

Llansola, M., Sanchez-Perez, A., Cauli, O., Felipo, V., 2005. Modulation of NMDA receptors in the cerebellum. 1. Properties of the NMDA receptor that modulate its function. Cerebellum (London, England) 4 (3), 154–161.

Maestri, L., Negri, S., Ferrari, M., Ghittori, S., Fabris, F., Danesino, P., Imbriani, M., 2006. Determination of perfluorooctanoic acid and perfluorooctanesulfonate in human tissues by liquid chromatography/single quadrupole mass spectrometry. Rapid Commun. Mass Spectrom. 20 (18), 2728–2734.

Marini, A.M., Paul, S.M., 1992. N-methyl-D-aspartate receptor-mediated neuroprotection in cerebellar granule cells requires new RNA and protein synthesis. Proc. Natl. Acad. Sci. U. S. A. 89 (14), 6555–6559.

Mariussen, E., Myhre, O., Reistad, T., Fonnum, F., 2002. The polychlorinated biphenyl mixture aroclor 1254 induces death of rat cerebellar granule cells: the involvement of the N-methyl-D-aspartate receptor and reactive oxygen species. Toxicol. Appl. Pharmacol. 179 (3), 137–144.

Mitsui, T., Neuhuber, B., Fischer, I., 2011. Acute administration of AMPA/Kainate blocker combined with delayed transplantation of neural precursors improves lower urinary tract function in spinal injured rats. Brain Res. 1418, 23–31.

Mosmann, T., 1983. Rapid colorimetric assay for cellular growth and survival: application to proliferation and cytotoxicity assays. J. Immunol. Methods 65 (1–2), 55–63.

Nilsson, H., Karrman, A., Westberg, H., Rotander, A., van Bavel, B., Lindstrom, G., 2010. A time trend study of significantly elevated perfluorocarboxylate levels in humans after using fluorinated ski wax. Environ. Sci. Technol. 44 (6), 2150–2155.

OECD, 2009. PFCs: Outcome of the 2009 survey. Survey on the production, use and release of PFOS, PFAS, PFOA, PFCA, their related substances and products/mixtures containing these substances. Paris.

Olsen, G.W., Burris, J.M., Ehresman, D.J., Froehlich, J.W., Seacat, A.M., Butenhoff, J.L., Zobel, L.R., 2007. Half-life of serum elimination of perfluorooctanesulfonate,perfluorohexanesulfonate, and perfluorooctanoate in retired fluorochemical production workers. Environ. Health Perspect. 115 (9), 1298–1305.

Paoletti, P., Bellone, C., Zhou, Q., 2013. NMDA receptor subunit diversity: impact on receptor properties, synaptic plasticity and disease. Nat. Rev. Neurosci. 14 (6), 383–400.

Reistad, T., Mariussen, E., Ring, A., Fonnum, F., 2007. In vitro toxicity of tetrabromobisphenol-A on cerebellar granule cells: cell death, free radical formation, calcium influx and extracellular glutamate. Toxicol. Sci. 96 (2), 268–278.

Rojas, D.C., 2014. The role of glutamate and its receptors in autism and the use of glutamate receptor antagonists in treatment. Journal of neural transmission (Vienna, Austria: 1996) 121 (8), 891–905.

Roth, N., Wilks, M.F., 2014. Neurodevelopmental and neurobehavioural effects of polybrominated and perfluorinated chemicals: a systematic review of the epidemiological literature using a quality assessment scheme. Toxicol. Lett. 230 (2), 271–281.

Sattler, R., Xiong, Z., Lu, W.Y., Hafner, M., MacDonald, J.F., Tymianski, M., 1999. Specific coupling of NMDA receptor activation to nitric oxide neurotoxicity by PSD-95 protein. Science 284 (5421), 1845–1848.

Schmidt, R.J., Lyall, K., Hertz-Picciotto, I., 2014. Environment and Autism: Current State of the Science. Cutting edge psychiatry in practice 1 (4), 21–38.

Schramm, M., Eimerl, S., Costa, E., 1990. Serum and depolarizing agents cause acute neurotoxicity in cultured cerebellar granule cells: role of the glutamate receptor responsive to N-methyl-D-aspartate. Proc. Natl. Acad. Sci. U. S. A. 87 (3), 1193–1197.

Strandabo, R.A., Gronlien, H.K., Ager-Wick, E., Nourizadeh-Lillabadi, R., Hildahl, J.P., Weltzien, F.A., Haug, T.M., 2016. Identified lhb-expressing cells from medaka (Oryzias latipes) show similar Ca(2 +)-response to all endogenous Gnrh forms, and reveal expression of a novel fourth Gnrh receptor. Gen. Comp. Endocrinol. 229, 19–31.

Swerea, I.V.F., 2009. Survey, Screening and Analyses of PFCs in Consumer Products. Mölndal, Sweden.

Tarnok, K., Czondor, K., Jelitai, M., Czirok, A., Schlett, K., 2008. NMDA receptor NR2B subunit over-expression increases cerebellar granule cell migratory activity. J. Neurochem. 104 (3), 818–829.

UNEP, 2010. The 9 new POPs. An introduction to the nine chemicals added to the Stockholm Convention by the Conference of the Parties at its fourth meeting.

Vallano, M.L., Lambolez, B., Audinat, E., Rossier, J., 1996. Neuronal activity differentially regulates NMDA receptor subunit expression in cerebellar granule cells. J. Neurosci. 16 (2), 631–639.

Volbracht, C., van Beek, J., Zhu, C., Blomgren, K., Leist, M., 2006. Neuroprotective properties of memantine in different in vitro and in vivo models of excitotoxicity. Eur. J. Neurosci. 23 (10), 2611–2622.

Volpe, J.J., 2009. Cerebellum of the premature infant: rapidly developing, vulnerable, clinically important. J. Child Neurol. 24 (9), 1085–1104.

Watanabe, M., Mishina, M., Inoue, Y., 1994. Distinct spatiotemporal expressions of five NMDA receptor channel subunit mRNAs in the cerebellum. J. Comp. Neurol. 343 (4), 513–519.

Xia, Y., Ragan, R.E., Seah, E.E., Michaelis, M.L., Michaelis, E.K., 1995. Developmental expression of N-methyl-D-aspartate (NMDA)-induced neurotoxicity, NMDA receptor function, and the NMDAR1 and glutamate-binding protein subunits in cerebellar granule cells in primary cultures. Neurochem. Res. 20 (5), 617–629.

Yang, X., Wang, L., Sun, W., Xue, Z., 2009. Effects of perfluorooctane sulfonate on amino acid neurotransmitters and glutamine synthetase in rats. Wei sheng yan jiu = Journal of hygiene research 38 (1), 19–21.